AAAS
Journal of Remote Sensing
Volume 2021, Article ID 8379391, 14 pages
https://doi.org/10.34133/2021/8379391

Journal of Remote Sensing
A SCIENCE PARTNER JOURNAL

Review Article

Mapping Crop Phenology in Near Real-Time Using Satellite Remote Sensing: Challenges and Opportunities

Feng Gao[1] **and Xiaoyang Zhang**[2]

[1]*USDA Agricultural Research Service, Hydrology and Remote Sensing Laboratory, 10300 Baltimore Avenue, Beltsville, MD 20705, USA*
[2]*Geospatial Sciences Center of Excellence, Department of Geography and Geospatial Sciences, South Dakota State University, Brookings, SD 57007, USA*

Correspondence should be addressed to Feng Gao; feng.gao@usda.gov

Received 13 November 2020; Accepted 23 February 2021; Published 24 March 2021

Crop phenology is critical for agricultural management, crop yield estimation, and agroecosystem assessment. Traditionally, crop growth stages are observed from the ground, which is time-consuming and lacks spatial variability. Remote sensing Vegetation Index (VI) time series has been used to map land surface phenology (LSP) and relate to crop growth stages mostly after the growing season. In recent years, high temporal and spatial resolution remote sensing data have allowed near-real-time mapping of crop phenology within the growing season. This paper summarizes two classes of near-real-time mapping methods, i.e., curve-based and trend-based approaches. The curve-based approaches combine the time series VIs and crop growth stages from historical years with the current observations to estimate crop growth stages. The curve-based approaches are capable of a short-term prediction. The trend-based approaches detect upward or downward trends from time series and confirm the trends using the increasing or decreasing momentum and VI thresholds. The trend-based approaches only use current observations. Both curve-based and trend-based approaches are promising in mapping crop growth stages timely. Nevertheless, mapping crop phenology near real-time is challenging since remote sensing observations are not always sensitive to crop growth stages. The accuracy of crop phenology detection depends on the frequency and availability of cloud-free observations within the growing season. Recent satellite datasets such as the harmonized Landsat and Sentinel-2 (HLS) are promising for mapping crop phenology within the season over large areas. Operational applications in the near future are feasible.

1. Introduction

Crop phenology defines physiological development stages of crop growth from planting to harvest. Crop growth management and yield estimation require accurate crop phenology information during the growing season [1]. For example, water stress in different crop growth stages may impact crop yield differently [2, 3]. For this reason, irrigation may be scheduled depending on the crop growth stage. Some crop growth stages, such as the latter part of the reproductive growth stages for soybeans and the earlier tasseling period for corn, are more beneficial for irrigation application. Crop phenology can also be used for fertilization scheduling, pest management, and harvesting operation. Crop phenology and growth condition provide information for crop growth modeling and yield estimation [4].

Crop phenology (growth stage) varies by year and location and is affected by climate variation, local weather, soil properties, and anthropogenic activities. The crop growth stage starts with planting or emergence and ends with the harvest. Crop planting dates depend on soil temperature, soil moisture, weather condition, and farmer practices. Wet weather may delay crop planting. In 2019, corn planting dates in the United States (U.S.) Corn Belt (Midwestern states) were delayed for about 1-2 weeks in Iowa and 3-4 weeks in Illinois compared to the 5-year average due to heavy springtime precipitation [5]. In this case, farmers switched crops from corn to soybean or other later-growing crops. Some fields could not be planted due to the inclement weather and were covered by the federal crop insurance. After planting, emergence is the first vegetative growth stage and the first predictor of crop success. Knowing the crop

emergence at the early growing period is critical for early crop mapping and crop condition monitoring. Harvest is the last growth stage and represents the end of the season for crops. The harvest dates may vary on the weather condition and equipment availability. The emergence and harvest dates define the crop growing period for biomass and yield production. Other crop growth stages during the growing period differ among crop types. In the United States, the U.S. Department of Agriculture (USDA) National Agricultural Statistics Service (NASS) publishes crop growth stages weekly at district (multicounties) or state level based on ground observations. Corn in the Corn Belt region is usually planted in late April to early June, while the usual harvest time for corn spanned from middle September to middle November [6].

Winter cover crops have been recognized as an important component of watershed conservation implementation plans to achieve water quality goals [7]. For example, in the lower Chesapeake Bay (LCB) in the Delmarva peninsula, eastern shore of U.S., cost-share programs have been established to encourage the planting of cover crops for reducing nutrient and sediment losses from farmland and for achieving water quality objectives [8]. The programs require that cover crops be planted and terminated within a specified time window. In the 2019-2020 winter cover crop management agreement, the Maryland Department of Agriculture cost-share program requires that cover crops terminate/eradicate between March 1, 2020, and June 14, 2020 [8]. The terminations after May 1 are encouraged and will receive additional payments for higher nutrition uptake. Traditionally, farmers report the cover crop termination dates, and conservation district staffs confirm the report through field surveys. The process is labor-intensive and time-consuming. For operational winter cover crop assessment, cover crop phenology such as emergence and termination dates is needed in weeks or even days.

Satellite remote sensing provides frequent observations of land surface properties, which can characterize crop and vegetation phenology. Phenological timing and magnitude are frequently derived from satellite spectral Vegetation Indices (VIs), representing the seasonal dynamics of vegetation community in a pixel instead of the features of a specific plant. For distinguishing field-based observations of plant phenology, satellite-derived phenological dynamics are often referred to as land surface phenology (LSP) [9–11] or simply remote sensing phenology [12]. LSP products may include VI metrics and phenological dates. The VI metrics provide VI values at the specific phenological dates, as well as other time series features such as minimum, maximum, amplitude (the difference between maximum and minimum), or the integral of VI during a period. In this paper, we focus on phenological dates. Once phenological dates are determined, the VI metrics are straightforward to generate using the VI time series.

Remote sensing phenology or LSP may use different terminologies, such as greenup vs. start of the season and dormancy vs. end of the season. This paper uses terminology inherited from MODIS and VIIRS data products (i.e., greenup onset, maturity onset, senescence onset, and dormancy onset). However, remote sensing phenological dates are different from crop growth stages. The greenup event may be related to emergence, and dormancy onset may be related to harvest. Their connections depend on crop types and the remote sensing phenology method used [12]. Remote sensing phenology is determined by the change of green vegetation status observed from remote sensing sensors. Such change could be related to the fitting function's inflection point or a certain level of change in the VI time series [12]. Crop growth stages are reported according to physiological growth stages. They are observed from the ground by trained observers [5]. Phenocams can provide information for certain growth stages but still cannot replace ground observations. Table 1 lists the key crop growth stages for corn and soybean in the USDA NASS crop progress reports and their possible relations to remote sensing phenology. In Table 1, land surface phenology from remote sensing includes greenup onset, midgreenup phase, maximum greenup onset, senescence onset, midsenescence onset, and dormancy onset, which are detected based on the changes of the VI time series [10–14]. Not all crop growth stages can be directly related to LSP from remote sensing.

LSP has been detected from a variety of satellite observations. Among satellite remote sensing sensors, the Landsat Multispectral Scanner (MSS) is the first space-borne sensor that was launched in 1972 for characterizing the seasonality of vegetation [15]. However, the 16-day repeat cycle of Landsat observations is not well suitable for monitoring vegetation phenology. Remote sensing phenology or LSP detections only became applicable after daily satellite observations were available since 1981 from the Advanced Very High-Resolution Radiometer (AVHRR) [16].

LSP at a spatial resolution of 1-8 km has been widely derived from AVHRR data for climate trend analyses during the past four decades [13, 17–20]. The widely used AVHRR datasets include (1) global biweekly 8 km Normalized Difference Vegetation Index (NDVI) (since 1981) from NASA's Global Inventory Modeling and Mapping Studies (GIMMS) [21], (2) 10-day 1 km NDVI (since 1989) over the contiguous United States from USGS (U.S. Geological Survey) EROS (Earth Resources Observation and Science) Data Center [22], (3) weekly 4 km Global Vegetation Index (GVIx) product (since 1981) from NOAA NESDIS (National Environmental Satellite, Data, and Information Service) [23], and (4) daily 5 km NDVI (since 1981) globally from the NASA Long-Term Data Record (LTDR) [24]. LSP has also been extracted using a 10-day 1 km *Satellite Pour l'Observation de la Terre* (SPOT) Vegetation (VGT) sensor, available from 1998 to 2014 [25, 26].

LSP at 250 m–1000 m pixels has been increasingly produced with the availability of Moderate Resolution Imaging Spectroradiometer (MODIS) onboard TERRA (launched in 1999) and AQUA (launched in 2001) [27–29]. For LSP detections, NDVI and Enhanced Vegetation Index (EVI) are commonly computed from MODIS Nadir bidirectional reflectance distribution function- (BRDF-) adjusted reflectance (NBAR) products (daily or 8 days at 500 m) [14, 30] and Vegetation Index products (16-day composite at 250 m, 500 m, and 1000 m) [28, 31]. Similarly, LSP has also been detected from the Visible/Infrared Imager/Radiometer Suite (VIIRS) that builds on MODIS and AVHRR heritage [32].

Table 1: Key crop growth stages and description for corn and soybean (adopted from USDA NASS) and remote sensing phenology (LSP).

Corn	Description	Soybean	Description	Phenology from remote sensing
Planting	When the seeds are placed in the ground	Planting	When the seeds are placed in the ground	No detection, but correlate to greenup onset or midgreenup phase
Emergence	As soon as the plants are visible	Emergence	As soon as the plants are visible	Greenup onset (or correlate to midgreenup phase)
Silking	The emergence of silk-like strands from the end of ears	Blooming	As soon as one bloom appears	Maximum greenness onset
Dough	Half of the kernels show dent with some thick or dough-like substance in all kernels	Setting pods	Pods develop on the lower nodes, with some blooming still occurring on the upper nodes	Senescence onset
Dent	All kernels are fully dented and the ear is firm and solid, but no milk present in most kernels	Turning yellow	Leaves of soybean start to turn yellow	Between senescence onset and midsenescence onset
Mature	Safe from frost and is about ready to harvest with shucks opening, no green foliage present	Dropping leaves	Leaves near the bottom of the plant are yellow and dropping, while leaves at the very top may still be green, leaves are 30-50 percent yellow	Midsenescence onset
Harvest	Cut, threshed, or gathered from the field	Harvest	Cut, threshed, or gathered from the field	Dormancy onset

For improving the spatial resolution for relatively homogeneous pixels, LSP at 30 m or finer pixels has been recently retrieved from Landsat, Sentinel-2, the harmonized Landsat and Sentinel-2 (HLS) [12, 33–40], and the Vegetation and Environment monitoring New MicroSatellite (VENμS) [35, 41]. To improve the temporal resolution in the time series with fewer cloud contaminations, LSP was detected from the new generation of geostationary satellites that provides red and near-infrared reflectances at a revisit frequency of 5-15 minutes [42].

Most of the satellite LSP products are produced annually. They are generated in a few months to a year after the growing season. Retroactive LSP products are mainly used for research purposes. They are not suitable for operational applications that need crop phenology information within the season, usually a few days or weeks after the change of crop growth stages. This paper defines the near-real-time term, similar to the crop progress reporting interval, ranging from a few days to weeks required by operational applications and statistics purposes. From the data production point of view, the total time of detection depends on the latency of satellite observations and the time needed to confirm phenology in the remote sensing phenology algorithm. From the algorithm point of view, the real-time or near-real-time approaches do not require a full year of data and can run as soon as remote sensing observations become available. Real-time or near-real-time algorithms depend on data availability and may not produce real-time or near-real-time data products.

The after-season phenology mapping approaches and LSP data products have been reviewed in several publications [40, 43, 44]. Misra et al. summarized general phenological research using Sentinel-2 and discussed future improvements [40]. Zeng et al. summarized methods for LSP detection and focused on the after-season approaches [43]. Berra and Gaulton examined LSP studies related to temperate and boreal forests [44]. The objective of this paper is to present the latest advancement in crop phenology mapping in near real-time using multisource satellite images. Opportunities, challenges, and future development for the near-real-time crop phenology mapping are discussed.

2. Crop Phenology Mapping Methods

2.1. Classification of Remote Sensing Approaches. Remote sensing phenology mapping approaches may be categorized in different ways. From the data production point of view, the methods can be classified as after-season and within-season approaches. After-season approaches have been used in producing LSP annual products, including from MODIS, VIIRS, and HLS [14, 32, 33]. The MODIS land cover dynamic product (MCD12Q2) uses three consecutive years of MODIS time series to produce LSP for the middle year [30]. The VIIRS and HLS use two years of time series data, i.e., the year of interest plus 6 months of Vegetation Index prepended and appended [32, 33]. The after-season LSP products are produced in 6 months to 1 year after the growing season. They usually cover a complete cycle of vegetation growth and include a full LSP from greenup to dormancy. The within-season approaches use the latest available remote sensing observations to produce LSP using any period of time series data. Since the within-season approaches can run any time using the latest observations, they are also referred to as real-time or near-real-time approaches [45]. A near-real-time approach has been developed to monitor vegetation (including crop) growth at 500 m pixels using MODIS and

VIIRS data [45–47]. Recently, within-season approaches have been developed to map crop phenology at the field scale using VENμS, Sentinel-2, and HLS datasets [35, 41]. The within-season approaches are aimed at producing the specific crop growth stages (e.g., emergence or harvest dates) near real-time for operational applications.

Recent within-season phenology approaches can be categorized as curve-based and trend-based approaches. The curve-based approaches require vegetation development information from historical years as ancillary information for the current year. They are also called reference-based approaches [48]. In these approaches, the standard curves for the same land cover type from historical years are used to match remote sensing observations from the current year. Sakamoto et al. [49, 50] developed a two-step filtering approach to detect maize and soybean phenology using a shape model from MODIS Wide Dynamic Range Vegetation Index (WDRVI). The crop-specific shape serves as a priori information to fit observed MODIS WDRVI data using scale and shift parameters. Crop growth stages were estimated once the parameters are determined [49–51]. Sun et al. extended a similar idea to fuse MODIS and Landsat/Sentinel-2 data [48]. The annual NDVI curves from MODIS were used to fit observed Landsat and HLS data for the same crop type. The fused data were then used to estimate crop phenology at 30 m resolution. Zhang et al. proposed an approach to monitor vegetation phenology in real time and forecast it in the short term ahead by combining timely available satellite observations with the climatology of vegetation phenology [45]. Liu et al. used this approach to monitor corn and soybean phenology in the Midwestern United States in 2014 and 2015 using MODIS and VIIRS [47]. The curve-based approaches use ancillary information of crop phenology and are robust under normal conditions.

Unlike the curve-based approach, the trend-based approaches only use recent remote sensing data observed from the current growing season. They search the changing trend from the VI time series and detect the transition dates that show a substantial change [13, 35, 41]. Reed et al. [13] used the Delayed Moving Average (DMA) approach to detect vegetation greenup within the season from the AVHRR time series. Gao et al. [35, 41] used the Moving Average Convergence Divergence (MACD) [35, 41] as an indicator to detect the increasing or decreasing trend in the VENμS, Sentinel-2, and HLS time series. The trend-based approaches do not depend on the crop curve or conditions from previous years and do not need crop type information. Since the trend-based approaches are based on the latest observations, they cannot predict phenology. We will describe both approaches and applications in detail in the following subsections.

From the technical point of view, LSP can be extracted by using the predefined thresholds, the curvature of time series, the adjustment from the previous phenology, and the changing trend. The threshold-based approaches use the VI values or the percentage of the amplitude VI as a predefined threshold [52], which was also used in the MODIS Collection 6 and HLS phenology data products [30, 33]. The curvature-based approaches use the curvatures of the fitting function to determine the inflection dates [14]. The MODIS Collection 5 and VIIRS LSP products used the curvature-based approach [46, 53]. The adjustment of previous phenology is a curve-based approach that uses the crop growth stages from previous years and then adjusts to the current year using timely available observations [45, 47–50]. Alternatively, the changing trend approaches use moving average techniques [13, 35, 41] to detect the increasing or decreasing trend in the VI time series.

2.2. Curve-Based Near-Real-Time Phenology Approach. Zhang et al. proposed a curve-based approach to monitor vegetation phenology in near real-time by combining timely available satellite observations with the climatology of vegetation phenology [45]. The approach has the capability of a short-term forecast, which is performed based on the following steps.

First, climatological phenometrics are detected from long-term satellite observations. The climatology could be derived from MODIS time series because this dataset is available since 2000 and was designed for monitoring land surface properties [54]. The phenometrics includes both phenological timing and phenological greenness. The phenological timing includes greenup onset, maturity onset, senescence onset, and dormancy onset. The phenological greenness is the greenness at greenup onset (close to the minimum greenness during a growing season), greenness at maturity onset (close to the maximum greenness during a growing season), and greenness during dormancy phase representing background condition. For each individual year, VI time series is reconstructed using the hybrid pieces logistic models (HPLM) [20]. The phenological timing is identified using the extreme values in the curvature change rate of HPLM [14], and the phenological greenness is then calculated from HPLM instead of raw VI time series. Using the phenometrics from the long-term MODIS time series, the climatology of a specific phenometric, which represents the potential range of vegetation greenness variations, is calculated using the mean value (MV) and standard deviation (SD) for the metrics separately.

Second, the potential temporal VI trajectories are simulated in near real-time. For a given day (the time of the latest satellite observation), the available VI observations are combined with the climatological phenometrics to simulate the temporal VI trajectory for a greenup phase or senescence phase using HPLM [45, 47] (Figure 1). A set of potential temporal VI trajectories are simulated using the HPLM at the time at each VI observation with the climatological phenometrics varying between MV-SD and MV+SD. The interval of climatological variation is set as 0.002 in phenological greenness and one day in phenological timing. This process is conducted separately for greenup phase and senescence phase.

Third, the simulation of potential temporal trajectories starts when the following criteria are met for the greenup or senescence phases. During the greenup phase, the criteria for the starting date are as follows: (1) a date for a given year could be as early as one month before the climatology of greenup onset; (2) land surface temperature (LST) is larger than 278 K (5°C) [45]; and (3) VI is larger than background

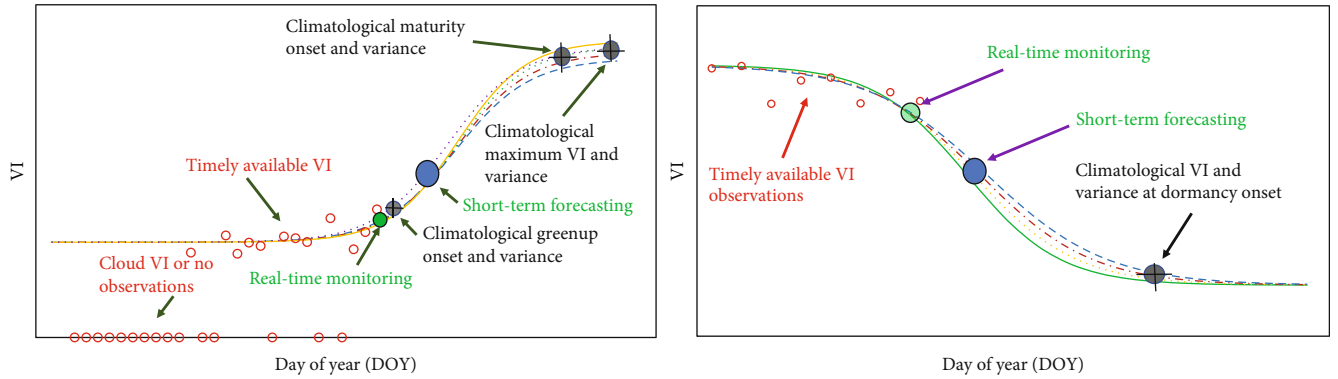

FIGURE 1: A scheme for monitoring phenology in near real-time and short-term forecasting from timely available satellite observations for (a) spring vegetation growing phase and (b) autumn senescence phase. The red circles are the VI data available at the time of simulating the temporal trajectories. The black bar represents the potential range of VI values at the climatological phenology timing. The trajectories are calculated from the available observations and the climatological VI. The curves are potential trajectories varying with the standard deviation in climatology (modified from Zhang [46]).

values with an increase of >0.02 during the consecutive two 3-day periods [47]. During the senescence phase, the criteria are as follows: (1) the date for a given year is one month earlier than climatology of senescence onset; and (2) VI is smaller than maximum values with a decrease of 0.02 for the consecutive two 3-day periods [47].

Fourth, phenological values are calculated for real-time monitoring and short-term forecasting. From a set of potential VI trajectories for a given day, a set of phenometrics are detected. Their mean value is taken as the prediction, and the standard deviation is considered as uncertainty. The prediction before the occurrence of a phenological event is called "short-term forecasting," while detection around the phenological occurrence is called "real-time monitoring." After passing a phenological event, the detection is defined as "near-real-time monitoring."

The vegetation monitoring from satellite data is continuously conducted during the period of vegetation development. The second to fourth steps are repeated every 3 days for the real-time monitoring and short-term forecasting of phenology with the accumulation of satellite observations.

2.3. Trend-Based Near-Real-Time Approaches. Trend-based approaches only use available observations from the current growing season [13]. They target the specific crop growth stages, such as emergence and harvest, for operational applications. Two approaches have recently been developed to map within-season crop emergence (WISE) [35] and within-season crop termination (WIST) [41]. Both approaches can run in near real-time using a partial year of observations. The processes include three steps.

First, the discrete remote sensing observations are smoothed and gap-filled using a local moving Savitzky–Golay (SG) filter. Clouds, cloud shadows, and low-quality remote sensing data are excluded from the processing. Since clear observations are unevenly distributed and some periods have a large temporal gap than others, a flexible sampling strategy is considered to fill large temporal gaps while keeping small variations in time series. The flexible sampling strategy considers the number of samples rather than the fixed window size used in the original SG filtering approach. Thus, the flexible sampling strategy uses a small moving window size for the time that has frequent observations and enables a large moving window for the time with fewer observations. In this way, a large temporal gap can be filled using a large moving window, while local variations can be preserved using a small moving window [35]. The SG filter is a local moving window approach and can be applied to any time series, no matter a few weeks or months. It has less assumption on the shape of time series than other mathematical functions used in phenology algorithms, such as harmonic regression, asymmetric Gaussian, and double logistic functions. The SG filter can remove noises (spikes) in time series and is an effective approach for generating a complete time series [55].

Once the smoothed and gap-filled time series is generated, the second step is to determine the significance of the trend. The trend-based approaches use the Moving Average Convergence Divergence (MACD) technique that has been used as an indicator to track the change of stock prices [56]. Figure 2 illustrates MACD terms and changing trends detected using the VENμS time series. The VENμS satellite is an experimental satellite and collects remote sensing images over the selected site in visible to near-infrared bands at 5 m resolution every two days [57]. The MACD time series is computed using the difference between two Exponential Moving Averages (EMA) with different lengths (periods) based on the smoothed and gap-filled time series VI. The short-term EMA ("a") tracks the rapid change of VI, and the long-term EMA ("b") tracks the slow changes. The differences (MACD) between two EMAs can capture the changing trend. Since MACD may be affected by small variations in NDVI time series, Gao et al. used the momentum threshold to determine a substantial upward or downward trend to distinguish a small variation from a meaningful change [35]. The momentum is computed as the cumulative values of MACD during the upward or downward period (blue-shaded areas in Figure 2). To confirm a trend, the cumulative

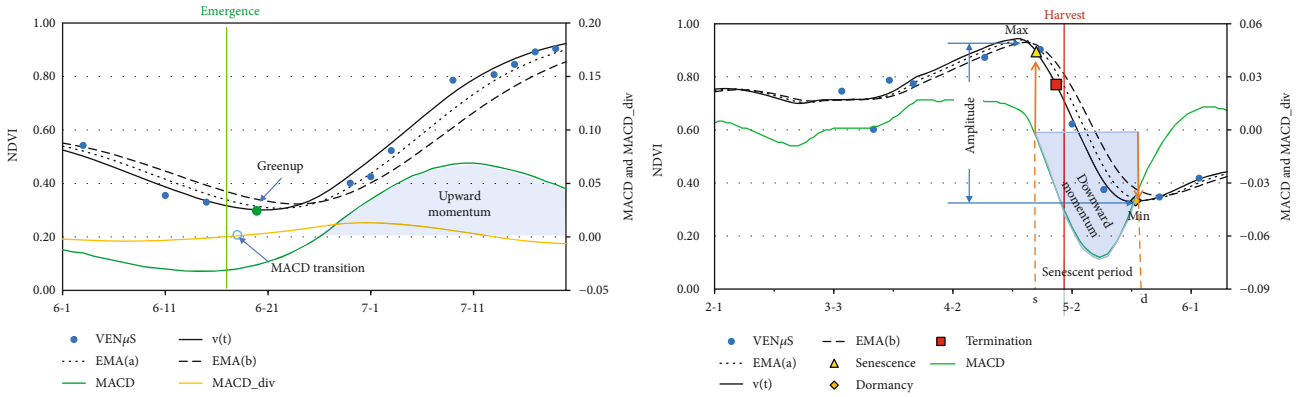

FIGURE 2: A diagram of NDVI (v(t)), EMA, MACD terms, and momentums shows the (a) greenup event and emergence and (b) senescence, dormancy, and the termination operation using VENμS time series (modified from Gao et al. [35, 41]). In addition to the MACD threshold, the trend-based approaches use the upward or downward momentums (blue-shaded areas) and VI amplitude to determine greenup and senescence events.

MACD must be larger than the predefined threshold. The threshold may depend on location and crop types. A lower threshold can capture small variations and detect a greenup event earlier. However, it may produce some false detections in the early stage. Once more observations become available, a greenup event (Figure 2(a)) can be confirmed by a large momentum. In addition to using the MACD threshold, the within-season termination (WIST) algorithm (Figure 2(b)) has a VI threshold that requires a substantial rate of decrease of VI during the senescent period for confirming a downward trend.

After a changing trend is confirmed, the third step uses the VI test to refine the phenology dates. For a greenup event (Figure 2(a)), the moving average of time series VI must show the increasing trend of VI. For cover crop termination/-harvest (Figure 2(b)), senescence and dormancy onsets are first detected during the downward (senescent) period. The termination dates are determined by the two observation dates that show the most rapid rate of decrease of VI during the senescent period (Figure 2(b)). By combining the changing trend and VI test, crop emergence and cover crop termination/harvest dates can be detected within 1-3 weeks after emergence and termination using VENμS time series [35, 41]. The WISE algorithm is a general approach and can be applied to many crops, including cover crops. The WIST algorithm is a more specific approach designed for detecting cover crop termination dates.

3. Applications Using Remote Sensing Phenology

3.1. Crop Growth Stages from VIIRS Using Curve-Based Approach. The HPLM-derived phenometrics provide a proxy of crop growth stages, although the six phenological timing metrics are not necessarily the same as the stages of crop development observed in the field (Table 1).

The HPLM for real-time monitoring of crop phenology was tested in the central United States [47]. First, climatological phenometrics were calculated from daily 500 m MODIS MCD43A4 product (Collection 6) from 2003 to 2012. The MCD43A4 provides 500 m daily Nadir BRDF-adjusted reflectance (*NBAR*). The two-band Enhanced Vegetation Index (EVI2) was calculated using red and near-infrared reflectance bands in the MCD43A4 product. The annual time series EVI2 was fitted to HPLM to retrieve historical phenometrics.

The timely available VIIRS observations were collected to monitor crop phenology in real time. The VIIRS observations were obtained from the NOAA VIIRS Environmental Data Record (EDR) products that are distributed through NOAA's CLASS (Comprehensive Large Array-Data Stewardship System) with a default latency of 6 hours. The products include daily spectral reflectance (375 m at nadir and 800 m at the scan edge in red and near-infrared reflectance), daily land surface temperature (LST), quality assessment (QA), and surface type containing dynamics of snow cover for each VIIRS granule. The VIIRS observations from granules were aggregated to 500 m grids using the nearest neighbor algorithm. Then, daily EVI2 was calculated and generated 3-day composites using maximum EVI2 from cloud-free observations.

Based on climatological phenometrics from MODIS and timely available VIIRS observations, the algorithm described in Section 2.2 was used to monitor corn and soybean phenology in 2014 and 2015 [47]. The real-time monitoring of greenup onset caused large uncertainty because the available VIIRS observations were limited and frequently contaminated by clouds. Therefore, the test was focused on real-time monitoring of the midday greenup phase and maturity onset (onset of greenness reaching maximum) (Figure 3), which was detected around the phenological occurrence (within ±3 days).

The results of real-time monitoring were comparable with the progress of growth stages from USDA NASS weekly crop progress reports across the Midwestern United States in both 2014 and 2015 [47]. The midgreenup phase monitored in real time was able to predict the planting dates of corn at each state with a lag of varying from 27 to 44 days and the

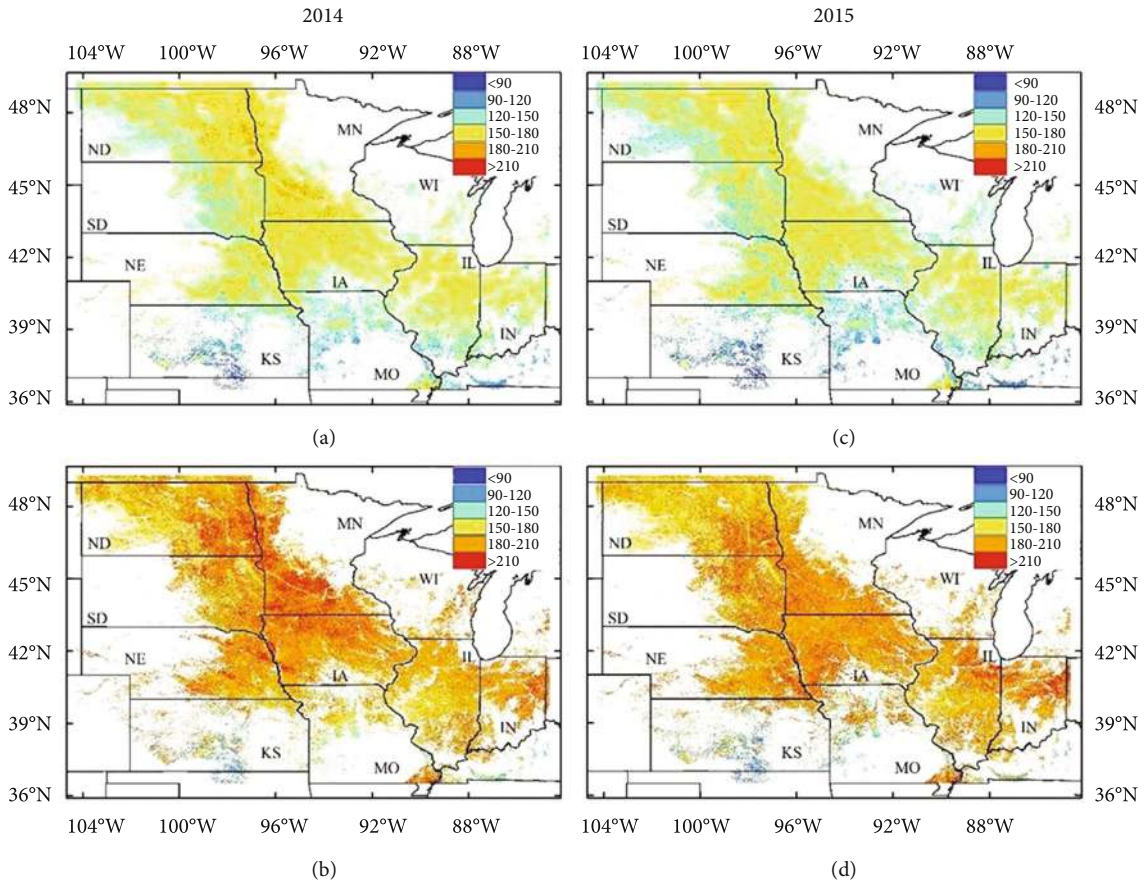

Figure 3: Spatial patterns in real-time monitoring of crop phenology (DOY, day of year) in the Midwestern United States in (a, b) 2014 and (c, d) 2015. (a, c) Midgreenup phase and (b, d) maximum greenness onset. ND: North Dakota; SD: South Dakota; NE: Nebraska; KS: Kansas; MN: Minnesota; IA: Iowa; MO: Missouri; WI: Wisconsin; IL: Illinois; IN: Indiana (adopted from Liu et al. [47]).

emergence dates that occurred with an early time from 15 to 31 days at different states. The VIIRS maturity onset (maximum greenness onset) was significantly correlated to the NASS corn silking dates with a lag of 8-11 days ahead. Similarly, real-time VIIRS phenology shows the capability of closely tracking NASS soybean progress. The midgreenup phase was able to estimate the planting date that occurred 22 to 39 days earlier and emergence dates that occurred from 12 to 26 days earlier in different states. The real-time monitoring of maximum greenness onset consistently indicated the soybean blooming dates with a lag of 1 to 14 days.

3.2. Within-Season Crop Emergence Using Trend-Based Approach. Crop emergence is hard to detect within the season (near real-time) since green vegetation changes over soil background are small at the pixel level. Using the within-season emergence (WSIE) approach described in Section 2.3, Gao et al. detected early crop greenup dates using VENμS observations (5 m, 2 days) [35]. The remote sensing greenup dates were within the early growth stages for corn and soybeans. The greenup dates were detected about 4-5 days after emergence, much earlier than the previous studies using curvature or threshold approaches. In those after-season approaches, greenup events were detected 2-4 weeks after emergence using the entire year of time series VI [12].

Figure 4 shows greenup dates detected using VENμS, Sentinel-2, and PlanetScope time series over the Beltsville Agricultural Research Center (BARC) experimental fields during the 2019 growing season. Greenups were mapped within two weeks after emergence using VENμS [35]. Sentinel-2 data (10 m, 5 days) detected the most greenup events, and results are close to those of VENμS. However, greenups for several fields in the BARC east were missing due to the lack of Sentinel-2 observations. BARC west locates in an overlapped area of two Sentinel-2 swathes and thus received more observations than BARC east. PlanetScope level 3 harmonized (L3H) data (3 m, 1 day) were used in this review for comparison. PlanetScope detected greenup events for crop fields similar to VENμS. More recent greenups were captured by PlanetScope L3H time series (Figure 4(c)) since the L3H data have been smoothed and gap-filled before using the WISE program. When enough clear observations are available, crop emergence dates detected from VENμS, Sentinel-2, and PlanetScope are close.

The routine HLS dataset [58] was also used to map crop emergence in the Choptank River watershed in the Delmarva peninsula, United States. The 30 m resolution remote sensing data are sufficient for agricultural landscapes in the U.S. [59]. The 3-4 days revisit for the combined Landsat-8 and Sentinel-2 data captured crop emergences for large fields 1-

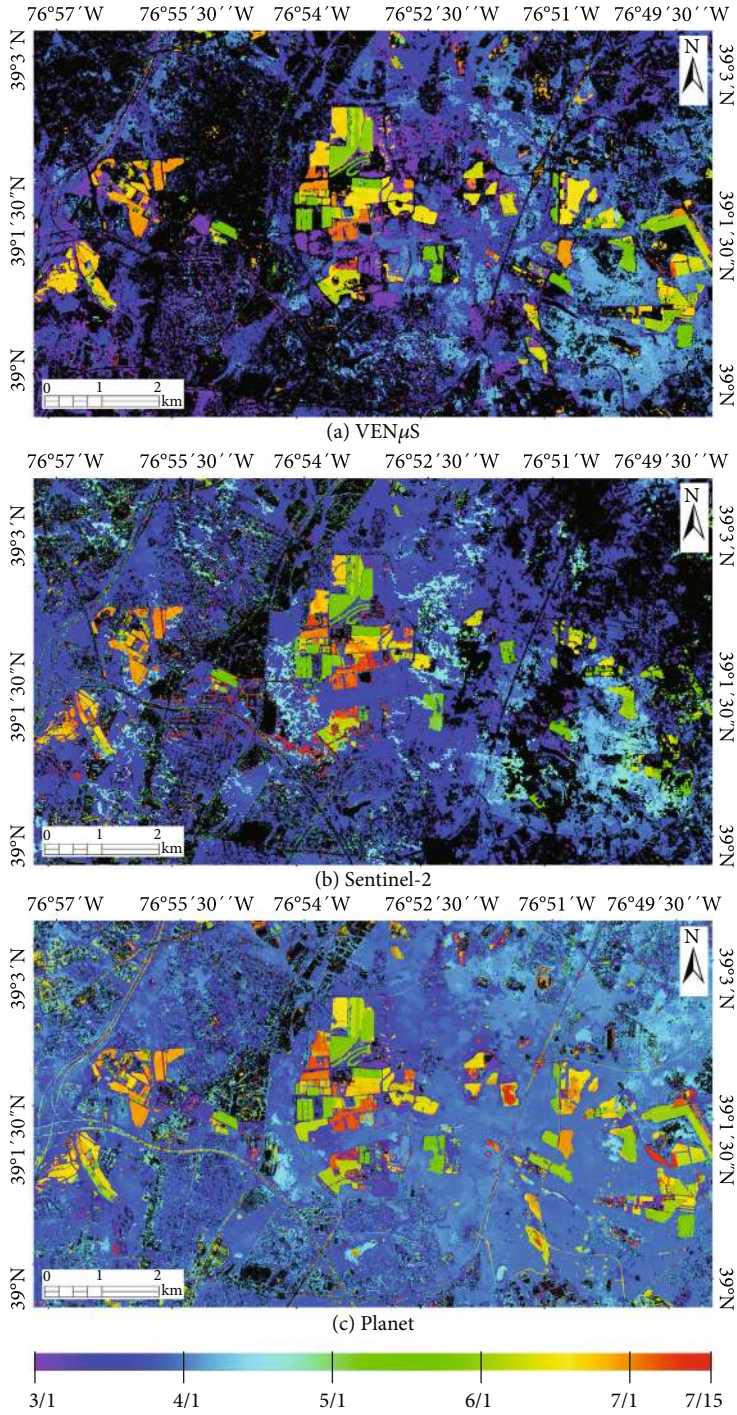

Figure 4: Greenup dates detected from (a) VENμS (modified from Gao et al. [35]), (b) Sentinel-2 (modified from Gao et al. [41]), and (c) PlanetScope time series over the Beltsville Agricultural Research Center (BARC) experimental fields in Beltsville, Maryland, USA, during the 2019 growing season. Satellite acquisitions from January 1, 2019, to July 27, 2019, were used to detect the most recent greenup events.

3 weeks after emergences [35]. In this review, we applied the WISE approach to the Corn Belt region. Figure 5 shows greenup dates from the WISE approach for the state of Iowa, USA, using HLS time series from January 1, 2018, to August 27, 2018. The remote sensing greenup dates detected within the growing season agree with the crop emergence dates reported by NASS. Figure 5 captures the spatial variability of crop emergences at the field scale across agricultural districts. Most of the fields have been mapped. Some pixels (black) were not mapped due to clouds or lacking clear observations. The stripes in Figure 5 are caused by the different numbers of observations from different satellite swathes.

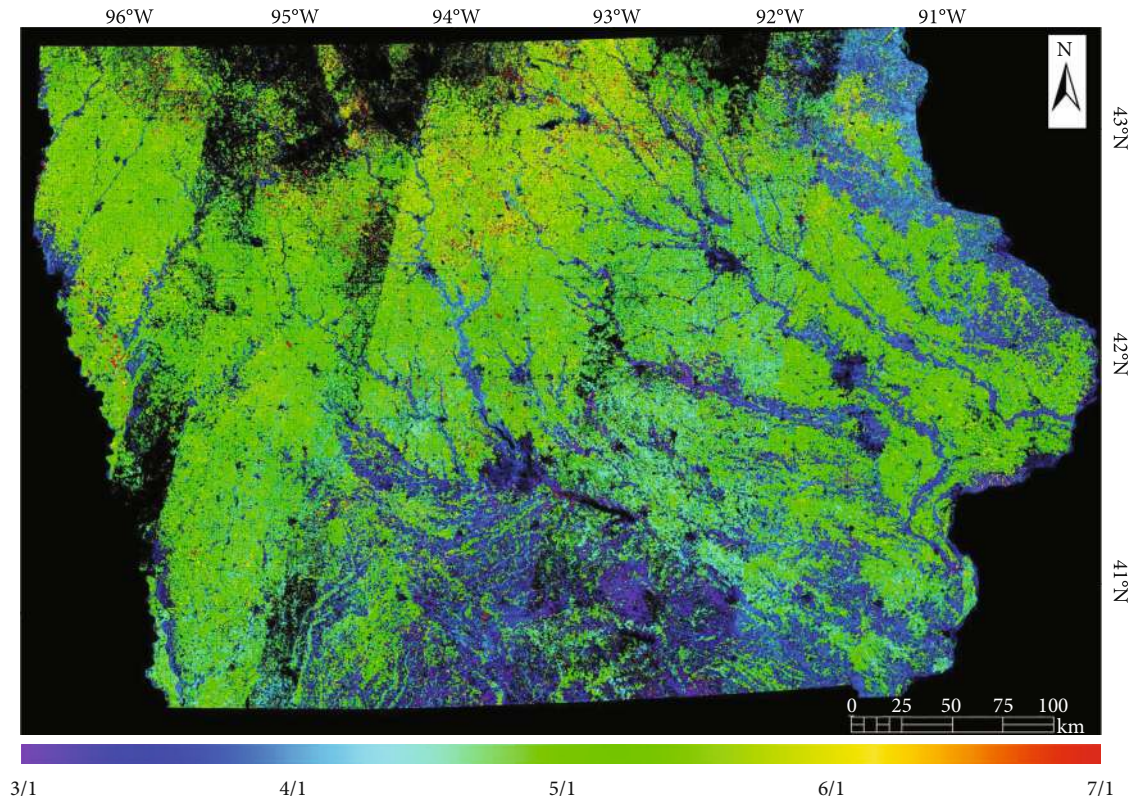

Figure 5: Greenup dates detected from HLS time series over the state of Iowa, USA, during the 2018 growing season using the WISE approach. Satellite acquisitions from January 1, 2018, to August 27, 2018, were used to detect the substantial greenup events.

The overlapped area from neighboring swathes received more observations and thus mapped crop emergence (greenup dates) more than other areas.

3.3. Within-Season Cover Crop Termination Using Trend-Based Approach. Cover crops are planted during the off-season. They are harvested/terminated when crops are green. Mapping cover crop termination using remote sensing at the field scale has been challenging due to the lack of suitable remote sensing data and methods.

Using the within-season termination (WIST) approach, Gao et al. detected cover crop termination dates from the BARC experimental fields in 2019 and 2020 [41]. Results show that termination dates detected using the VENμS time series NDVI agree with the harvest/termination operation records with a mean absolute difference of 2 days. The Sentinel-2 (5-day) time series also detected correct termination dates but with 7% missing and 10% false detections. A near-real-time simulation shows that the average delay times of detection were about 4-8 days after termination or harvest operations when satellite data have no delay. If considering the latency of satellite data, cover crop termination can be detected within 1-3 weeks. Figure 6 demonstrates the concept of near-real-time mapping of cover crop termination using remote sensing observations. In the weekly simulation, newly terminated/-harvested cover crops were detected by using recent satellite observations.

4. Discussions

4.1. Challenges. Mapping crop growth stages using remote sensing is challenging. LSP or remote sensing phenology is different from crop physiological growth stages. Remote sensing phenology needs to be correlated to crop growth stages for agricultural management. For operational applications, crop phenology mapping within the growing season (or near real-time) is required. There are several challenges to mapping crop growth stages in near real-time using remote sensing.

First, near-real-time mapping requires that remote sensing phenology approaches can detect crop growth stages using a partial year of remote sensing observations. In the early growth stages, crop emergence or early vegetative development may not be apparent at the pixel level in remote sensing images. The sensitivity of remote sensing signals to vegetative development depends on the characteristics of sensors such as bandwidths and signal-to-noise ratio. In crop phenology mapping, temporal consistency of time series remote sensing data is critical and required. During the early crop development, a small change of emergence may be complicated with the change of soil moisture, such as snow melting or rainfall. In addition, the availability of usable remote sensing observations is affected by clouds and thus affects phenology results [60]. For these reasons, near-real-time monitoring of crop emergence may be delayed. Recent studies show that crop emergence may be detected in 1-3 weeks

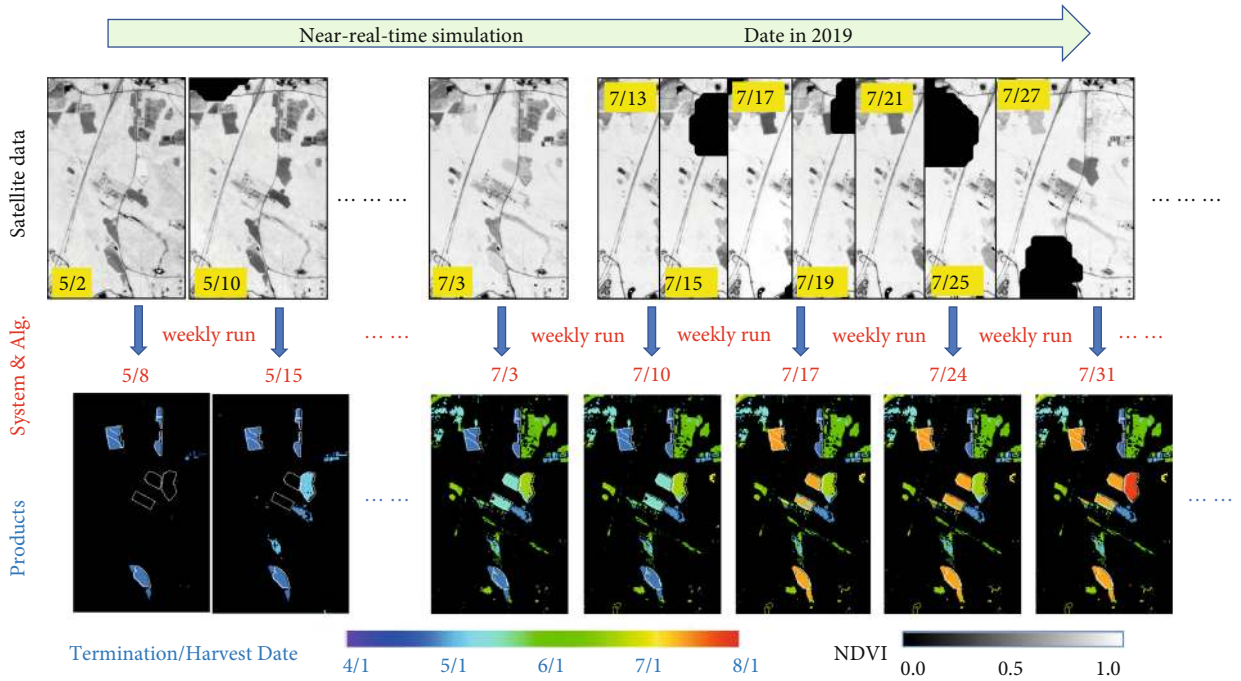

Figure 6: Near-real-time mapping of cover crop terminations using VENμS time series NDVI over BARC east, Maryland, USA. The timely available VENμS NDVI images in 2019 are shown in the upper panel. The newly detected termination dates for cover crop fields (based on Gao et al. [41]) are shown in the lower panel from the weekly simulation.

after emergence when green leaves have been developed, and the change of VI can be confirmed [35, 47].

Second, satellite observations are affected by many factors, and uncertainty always exists in an individual observation. These noises may come from the undetected clouds, cloud shadows, atmosphere effects, calibration errors, etc. The change of crop conditions from biotic and abiotic factors such as soil conditions, insect, and water stress may also affect VI time series. In the near-real-time mapping, a small variation in a few recent satellite observations may not reflect an actual change in crop growth conditions. As a result, the relative increase or decrease of vegetation greenness in the latest observation compared to previous values does not necessarily indicate actual vegetation greenness dynamics in the curve-based model. On the other hand, a real change signal may be mistreated as noise in reconstructing VI time series [61]. For example, alfalfa can be harvested a few times a year and regrow quickly after each harvest. If only 1 or 2 clear remote sensing observations capture the drop of VI, it will be a challenging case for phenology algorithms using optical remote sensing data to distinguish a real change of VI from a noise. In trend-based approaches, Gao et al. [35, 41] use the SG filter and require a minimum of 5 observations within ±60 days to fill temporal gaps. The combination of parameters captures all greenup and termination events for an alfalfa field in BARC using the 2-day revisit VENμS time series. The SG filter is more robust in capturing multiple growing seasons than the preassumed mathematical functions. However, when using the 5-day revisit Sentinel-2 time series, some greenup and termination events were missed. The capability of near real-time monitoring using optical remote sensing depends on crop type and satellite data used. High spatial resolution radar data may be an option to complement the optical remote sensing [62].

Third, crop growth stages may not be directly related to remote sensing phenology. For example, the within-season termination approach can detect terminations when cover crops are terminated in green. However, it cannot detect harvest dates for summer crops since the changes of VI are not substantial during the mature stages when leaves turn brown or yellow [41]. Remote sensing phenology or LSP has different relationships to the crop growth stages depending on crop types and methods used [63]. The curve-based approaches are useful to connect remote sensing phenology and crop growth stages based on remote sensing and ground observations from historical years [45–50]. However, the curve-based approaches usually require crop type information in the early growing season, which may not be available for most areas. The curve-based approaches assume the current year has a similar VI pattern to previous years. The assumption works for the normal years but may not work if crop condition changes due to biotic or abiotic reasons such as drought, floods, or insect damage. The trend-based approaches do not require crop type information but may be sensitive to small variations such as the growth of weeds. A hybrid model that combines information from remote sensing, crop growth knowledge, weather, and soil conditions may be a solution for crop growth monitoring near real-time.

Field observations are needed to associate remote sensing phenology with crop growth stages, especially after crop emergence. Previous validations mostly focused on a few stages using summarized statistics, such as the weekly NASS crop progress reports [12, 47, 49–51, 63]. The field-level

validation of crop growth stages is limited. In recent years, phenocams have been used to monitor vegetation phenology [64]. Phenocams network in the U.S. includes about 100 phenocams over agricultural sites [65], which is sparse and limited. For crop phenology monitoring, phenocams cannot replace ground observations since some crop growth stages cannot be observed from photos alone. Nevertheless, the near-surface phenocam network provides a way to validate land surface phenology and a quick assessment of crop growth stages and conditions. Ground observations of different crop physiological stages are needed for validation at the field level.

4.2. Opportunities. Previously, crop phenology mapping at field scale has been limited due to the lack of high temporal and spatial resolution data. These data from satellite remote sensing have become available in recent years. Several satellite constellations have provided the solution. For example, the two Sentinel-2 satellites (A and B) provide 10-20 m resolution imagery in visible and near-infrared bands every five days [66]. The harmonized Landsat and Sentinel-2 (HLS) dataset provides a global 30 m resolution surface reflectance product every 3-4 days since 2017 [58]. The commercial PlanetScope satellite constellation provides daily observations from a small satellite constellation at 3 m spatial resolution [67]. A recent study shows that crop emergence and cover crop harvest can be detected accurately using the 2-day revisit VENμS time series over BARC where about 25-30% clear pixels per day are available. The 5-day revisit Sentinel-2 detected emergence and harvest for most of the fields but with some missing and false detections. The harmonized Landsat and Sentinel-2 with a 3- to 4-day revisit can be used for a large area where field sizes are relatively large. As Landsat 9 and Sentinel-2C are scheduled to launch in 2021 and 2023, respectively, the medium-resolution Landsat and Sentinel-2 virtual constellation can provide continuous global observations every 1-2 days. Mapping crop phenology at the subfield to field scales in the near future is promising.

Data fusion approaches have been used to fill large temporal gaps using data sources in different spatial and temporal resolutions (e.g., polar-orbiting MODIS/VIIRS and Landsat/Sentinel-2) [68, 69] and for after-season crop phenology mapping [12, 38, 39]. The effectiveness of crop phenology mapping using data fusion depends on the availability of clear MODIS, Landsat, and Sentinel-2 images. In addition to polar-orbiting satellites, a new generation of geostationary satellites can image the Earth's surface every 10-15 min at 0.5-1 km spatial resolution. Geostationary observations provide more cloud-free observations and show the potential to improve LSP mapping [42, 70]. The geostationary data at coarse spatial resolution may be fused with the medium spatial resolution data (e.g., Landsat/Sentinel-2) to produce high temporal and spatial resolution data for crop phenology mapping at the field scale. Now, since high temporal and spatial resolution remote sensing observations are available, data fusion may not be critical for crop phenology mapping in near real-time for the region without persistent cloud cover, but further study is still needed. Data fusion is still a solution for crop phenology mapping for retroactive study, especially when frequent medium-resolution observations were not available in the early years.

Near-real-time remote sensing phenology approaches have been developed in recent years. They can be generalized for operational uses in agricultural management and agroecosystem services. The timely crop phenology provides information for irrigation and fertilization scheduling, crop condition monitoring, and yield estimation. Recent studies show that comparing VI or evapotranspiration at the same crop growth stages is more robust for crop condition monitoring and yield estimation than traditional approaches that compare VI at the same calendar date [4, 71]. Cover crop emergence and termination detected from remote sensing provide information for quantifying conservation practice implementation and enabling estimation of biomass accumulation [7, 8, 41].

5. Summary

Crop growth information is required for agricultural management and agroecosystem assessment. Remote sensing data have been used for mapping land surface phenology (LSP) and relating to crop growth stages. This paper reviews the within-season phenology mapping approaches that use timely available remote sensing observations to detect the recent crop phenological events in near real-time. Two groups of within-season approaches are presented. One group of methods uses time series shapes or curves from historical years and combines them with observations from the current year to estimate crop growth stages. Another group detects the changing trend and strength (momentum of change) using the latest available observations. Both approaches show promising results by comparing to the field observations and the summary of crop growth stages. However, near-real-time mapping of crop phenology is still very challenging since remote sensing observations may not be sensitive to the change of crop growth stages. Some crop growth stages may need a few days or weeks to confirm from the latest VI time series. Recent studies show that crop emergence and cover crop termination may be detected within 1-3 weeks after events when clear observations are available. As high temporal and spatial resolution satellite datasets such as the harmonized Landsat and Sentinel-2 (HLS) and PlanetScope become available, within-season or near-real-time crop phenology mapping at high (<10 m) to medium (10-30 m) spatial resolution is conceivable.

Disclosure

The funders had no role in the design of the study; in the collection, analyses, or interpretation of data; in the writing of the manuscript; or in the decision to publish the results. USDA is an equal opportunity provider and employer. Any use of trade, firm, or product names is for descriptive purposes only and does not imply endorsement by the U.S. Government.

Conflicts of Interest

The authors declare no conflict of interest.

Authors' Contributions

FG and XZ were responsible for conceptualization; FG and XZ were responsible for writing of the original draft; FG and XZ were responsible for writing, review, and editing. All authors have read and agreed to the published version of the manuscript.

Acknowledgments

The authors would like to thank Dr. Rasmus Houborg for providing Planet L3H data over BARC. The VENμS data were acquired and provided by the Israeli Space Agency and the Centre National d'Etudes Spatiales (CNES), France. The Sentinel-2 data were produced and provided by the European Space Agency (ESA). The harmonized Landsat and Sentinel-2 (HLS) data were produced by the National Aeronautics and Space Administration (NASA) Goddard Space Flight Center (GSFC). This research was a contribution from the Long-Term Agroecosystem Research (LTAR) network. LTAR is supported by the United States Department of Agriculture. This work was partially supported by the National Aeronautics and Space Administration (NASA) Land Cover and Land Use MuSLI program (NNH17ZDA001N-LCLUC) and the U.S. Geological Survey (USGS) Landsat Science Team program to FG. The research was also partially supported by the USDA grant GRANT12685068 and the NASA grant 80NSSC20K1337 to XZ.

References

[1] C. L. Walthall, J. Hatfield, P. Backlund et al., *Climate change and agriculture in the United States: effects and adaptation*, USDA Technical Bulletin 1935, Washington, DC, 2012, https://www.usda.gov/sites/default/files/documents/CC%20and%20Agriculture%20Report%20(02-04-2013)b.pdf.

[2] M. C. Anderson, C. R. Hain, F. Jurecka et al., "Relationships between the evaporative stress index and winter wheat and spring barley yield anomalies in the Czech Republic," *Climate Research*, vol. 70, no. 2, pp. 215–230, 2016.

[3] M. C. Anderson, C. Zolin, P. C. Sentelhas et al., "The evaporative stress index as an indicator of agricultural drought in Brazil: an assessment based on crop yield impacts," *Remote Sensing of Environment*, vol. 174, pp. 82–99, 2016.

[4] Y. Yang, M. C. Anderson, F. Gao et al., "Field-scale mapping of evaporative stress indicators of crop yield: an application over Mead, NE, USA, Nebraska," *Remote Sensing of Environment*, vol. 210, pp. 387–402, 2018.

[5] NASS, "Crop progress report," January 2021, http://www.nass.usda.gov/Publications/National_Crop_Progress/.

[6] NASS, *Usual planting and harvesting dates for U.S. field crops*, USDA NASS Agricultural Handbook No. 628, USDA NASS Agricultural Handbook No. 628, 1997https://www.nass.usda.gov/Publications/Todays_Reports/reports/fcdate10.pdf.

[7] W. D. Hively, M. Lang, G. W. McCarty, J. Keppler, A. Sadeghi, and L. L. McConnell, "Using satellite remote sensing to estimate winter cover crop nutrient uptake efficiency," *Journal of Soil and Water Conservation*, vol. 64, no. 5, pp. 303–313, 2009.

[8] Maryland Department of Agriculture, "2019/2020 Winter cover crop for nutrient management," January 2021, http://mda.state.md.us/resource_conservation/counties/FY20_Program%20Requirements%20and%20Agreement_website.pdf.

[9] K. M. de Beurs and G. M. Henebry, "Land surface phenology, climatic variation, and institutional change: analyzing agricultural land cover change in Kazakhstan," *Remote Sensing of Environment*, vol. 89, no. 4, pp. 497–509, 2004.

[10] M. Friedl, G. M. Henebry, B. Reed et al., "Land surface phenology. A Community White Paper requested by NASA," 2006, January 2021, https://cce.nasa.gov/mtg2008_ab_presentations/Phenology_Friedl_whitepaper.pdf.

[11] G. M. Henebry and K. M. de Beurs, "Remote sensing of land surface phenology: a prospectus," in *Phenology: An Integrative Environmental Science*, M. D. Schwartz, Ed., pp. 385–411, Springer, Dordrecht, 2013.

[12] F. Gao, M. C. Anderson, X. Y. Zhang et al., "Toward mapping crop progress at field scales through fusion of Landsat and MODIS imagery," *Remote Sensing of Environment*, vol. 188, pp. 9–25, 2017.

[13] B. C. Reed, J. F. Brown, D. VanderZee, T. R. Loveland, J. W. Merchant, and D. O. Ohlen, "Measuring phenological variability from satellite imagery," *Journal of Vegetation Science*, vol. 5, no. 5, pp. 703–714, 1994.

[14] X. Y. Zhang, M. A. Friedl, C. B. Schaaf et al., "Monitoring vegetation phenology using MODIS," *Remote Sensing of Environment*, vol. 84, no. 3, pp. 471–475, 2003.

[15] D. Thompson and O. Wehmanen, "Using Landsat digital data to detect moisture stress," *Photogrammetric Engineering and Remote-sensing*, vol. 45, pp. 201–207, 1979.

[16] S. Goward, C. Tucker, and D. Dye, "North American vegetation patterns observed with the NOAA-7 advanced very high resolution radiometer," *Vegetatio*, vol. 64, no. 1, pp. 3–14, 1985.

[17] R. de Jong, S. de Bruin, A. de Wit, M. E. Schaepman, and D. L. Dent, "Analysis of monotonic greening and browning trends from global NDVI time- series," *Remote Sensing of Environment*, vol. 115, no. 2, pp. 692–702, 2011.

[18] Y. Julien and J. A. Sobrino, "Global land surface phenology trends from GIMMS database," *International Journal of Remote Sensing*, vol. 30, no. 13, pp. 3495–3513, 2009.

[19] M. A. White, K. De Beurs, K. Didan et al., "Intercomparison, interpretation, and assessment of spring phenology in North America estimated from remote sensing for 1982-2006," *Global Change Biology*, vol. 15, no. 10, pp. 2335–2359, 2009.

[20] X. Y. Zhang, "Reconstruction of a complete global time series of daily vegetation index trajectory from long-term AVHRR data," *Remote Sensing of Environment*, vol. 156, pp. 457–472, 2015.

[21] J. E. Pinzon and C. J. Tucker, "A non-stationary 1981-2012 AVHRR NDVI3g time series," *Remote Sensing*, vol. 6, no. 8, pp. 6929–6960, 2014.

[22] J. C. Eidenshink, "The 1990 conterminous United-States Avhrr data set," *Photogrammetric Engineering and Remote Sensing*, vol. 58, pp. 809–813, 1992.

[23] F. Kogan, A. Gitelson, E. Zakarin, L. Spivak, and L. Lebed, "AVHRR-based spectral vegetation index for quantitative assessment of vegetation state and productivity,"

Photogrammetric Engineering and Remote Sensing, vol. 69, no. 8, pp. 899–906, 2003.

[24] J. Pedelty, S. Devadiga, E. Masuoka et al., "Generating a long-term land data record from the AVHRR and MODIS instruments," in *2007 IEEE International Geoscience and Remote Sensing Symposium*, pp. 1021–1025, Barcelona, Spain, 2007.

[25] N. Delbart, L. Kergoat, T. Le Toan, J. Lhermitte, and G. Picard, "Determination of phenological dates in boreal regions using normalized difference water index," *Remote Sensing of Environment*, vol. 97, no. 1, pp. 26–38, 2005.

[26] K. Bornez, A. Descals, A. Verger, and J. Penuelas, "Land surface phenology from VEGETATION and PROBA-V data. Assessment over deciduous forests," *International Journal of Applied Earth Observation and Geoinformation*, vol. 84, article 101974, 2020.

[27] S. Ganguly, M. A. Friedl, B. Tan, X. Y. Zhang, and M. Verma, "Land surface phenology from MODIS: characterization of the Collection 5 global land cover dynamics product," *Remote Sensing of Environment*, vol. 114, no. 8, pp. 1805–1816, 2010.

[28] B. Tan, J. T. Morisette, R. E. Wolfe et al., "An enhanced TIMESAT algorithm for estimating vegetation phenology metrics from MODIS data," *Ieee Journal of Selected Topics in Applied Earth Observations and Remote Sensing*, vol. 4, no. 2, pp. 361–371, 2011.

[29] X. Y. Zhang, M. A. Friedl, and C. B. Schaaf, "Global vegetation phenology from moderate resolution imaging spectroradiometer (MODIS): evaluation of global patterns and comparison with in situ measurements," *Journal of Geophysical Research-Biogeosciences*, vol. 111, no. G4, 2006.

[30] J. M. Gray, D. Sulla-menashe, and M. A. Friedl, "User Guide to Collection 6 MODIS Land Cover Dynamics (MCD12Q2) Product," 2019, https://lpdaac.usgs.gov/documents/218/mcd12q2_v6_user_guide.pdf.

[31] S. R. Karlsen, A. Tolvanen, E. Kubin et al., "MODIS-NDVI-based mapping of the length of the growing season in northern Fennoscandia," *International Journal of Applied Earth Observation and Geoinformation*, vol. 10, no. 3, pp. 253–266, 2008.

[32] X. Y. Zhang, S. Jayavelu, L. L. Liu et al., "Evaluation of land surface phenology from VIIRS data using time series of PhenoCam imagery," *Agricultural and Forest Meteorology*, vol. 256-257, pp. 137–149, 2018.

[33] D. K. Bolton, J. M. Gray, E. K. Melaas, M. Moon, L. Eklundh, and M. A. Friedl, "Continental-scale land surface phenology from harmonized Landsat 8 and Sentinel-2 imagery," *Remote Sensing of Environment*, vol. 240, article 111685, 2020.

[34] J. I. Fisher, J. F. Mustard, and M. A. Vadeboncoeur, "Green leaf phenology at Landsat resolution: scaling from the field to the satellite," *Remote Sensing of Environment*, vol. 100, no. 2, pp. 265–279, 2006.

[35] F. Gao, M. Anderson, C. Daughtry, A. Karnieli, D. Hively, and W. Kustas, "A within-season approach for detecting early growth stages in corn and soybean using high temporal and spatial resolution imagery," *Remote Sensing of Environment*, vol. 242, article 111752, 2020.

[36] C. P. Krehbiel, T. Jackson, and G. M. Henebry, "Web-enabled Landsat data time series for monitoring urban heat island impacts on land surface phenology," *Ieee Journal of Selected Topics in Applied Earth Observations and Remote Sensing*, vol. 9, no. 5, pp. 2043–2050, 2016.

[37] E. K. Melaas, M. A. Friedl, and Z. Zhu, "Detecting interannual variation in deciduous broadleaf forest phenology using Landsat TM/ETM \+ data," *Remote Sensing of Environment*, vol. 132, pp. 176–185, 2013.

[38] J. J. Walker, K. M. de Beurs, R. H. Wynne, and F. Gao, "Evaluation of Landsat and MODIS data fusion products for analysis of dryland forest phenology," *Remote Sensing of Environment*, vol. 117, pp. 381–393, 2012.

[39] X. Y. Zhang, J. Wang, G. M. Henebry, and F. Gao, "Development and evaluation of a new algorithm for detecting 30 m land surface phenology from VIIRS and HLS time series," *ISPRS Journal of Photogrammetry and Remote Sensing*, vol. 161, pp. 37–51, 2020.

[40] G. Misra, F. Cawkwell, and A. Wingler, "Status of phenological research using Sentinel-2 data: a review," *Remote Sensing*, vol. 12, no. 17, p. 2760, 2020.

[41] F. Gao, M. C. Anderson, and W. D. Hively, "Detecting cover crop end-of-season using VENμS and Sentinel-2 satellite imagery," *Remote Sensing*, vol. 12, no. 21, p. 3524, 2020.

[42] D. Yan, X. Y. Zhang, Y. Yu, and W. Guo, "A comparison of tropical rainforest phenology retrieved from geostationary (SEVIRI) and polar-orbiting (MODIS) sensors across the Congo Basin," *Congo Basin IEEE Transactions on Geoscience and Remote Sensing*, vol. 54, no. 8, pp. 4867–4881, 2016.

[43] L. Zeng, B. D. Wardlow, D. Xiang, S. Hu, and D. Li, "A review of vegetation phenological metrics extraction using time-series, multispectral satellite data," *Remote Sensing of Environment.*, vol. 237, article 111511, 2020.

[44] E. Berra and R. Gaulton, "Remote sensing of temperate and boreal forest phenology: a review of progress, challenges and opportunities in the intercomparison of in-situ and satellite phenological metrics," *Forest Ecology and Management*, vol. 480, article 118663, 2021.

[45] X. Y. Zhang, M. D. Goldberg, and Y. Y. Yu, "Prototype for monitoring and forecasting fall foliage coloration in real time from satellite data," *Agricultural and Forest Meteorology*, vol. 158, pp. 21–29, 2012.

[46] X. Y. Zhang, "3.05 - Land surface phenology: climate data record and real-time monitoring," in *Comprehensive Remote Sensing*, S. Liang, Ed., pp. 35–52, Elservier, New York, 2018.

[47] L. L. Liu, X. Y. Zhang, Y. Y. Yu, F. Gao, and Z. W. Yang, "Real-time monitoring of crop phenology in the Midwestern United States using VIIRS observations," *Remote Sensing*, vol. 10, no. 10, p. 1540, 2018.

[48] L. Sun, F. Gao, D. Xie et al., "Reconstructing daily 30 m NDVI over complex agricultural landscapes using a crop reference curve approach," *Remote Sensing of Environment*, vol. 253, article 112156, 2021.

[49] T. Sakamoto, B. D. Wardlow, A. A. Gitelson, S. B. Verma, A. E. Suyker, and T. J. Arkebauer, "A two-step filtering approach for detecting maize and soybean phenology with time-series MODIS data," *Remote Sensing of Environment*, vol. 114, no. 10, pp. 2146–2159, 2010.

[50] T. Sakamoto, B. D. Wardlow, and A. A. Gitelson, "Detecting spatiotemporal changes of corn developmental stages in the U.S. Corn Belt using MODIS WDRVI data," *IEEE Transactions on Geoscience and Remote Sensing*, vol. 49, no. 6, pp. 1926–1936, 2011.

[51] L. L. Zeng, B. D. Wardlow, R. Wang et al., "A hybrid approach for detecting corn and soybean phenology with time-series MODIS data," *Remote Sensing of Environment*, vol. 181, pp. 237–250, 2016.

[52] P. Jonsson and L. Eklundh, "Seasonality extraction by function fitting to time-series of satellite sensor data," *IEEE Transactions on Geoscience and Remote Sensing*, vol. 40, no. 8, pp. 1824–1832, 2002.

[53] X. Y. Zhang, M. A. Friedl, and G. M. Henebry, *VIIRS/NPP land cover dynamics yearly L3 global 500m SIN grid V001*, NASA EOSDIS Land Processes DAAC, 2020.

[54] C. O. Justice, J. R. G. Townshend, E. F. Vermote et al., "An overview of MODIS land data processing and product status," *Remote Sensing of Environment*, vol. 83, no. 1-2, pp. 3–15, 2002.

[55] J. Chen, P. Jonsson, M. Tamura, Z. H. Gu, B. Matsushita, and L. Eklundh, "A simple method for reconstructing a high-quality NDVI time-series data set based on the Savitzky-Golay filter," *Remote Sensing of Environment*, vol. 91, no. 3-4, pp. 332–344, 2004.

[56] G. Appel, *Technical Analysis Power Tools for Active Investors*, Financial Times Prentice Hall, 2005.

[57] G. Dedieu, O. Hagolle, A. Karnieli et al., "VENμS: performances and first results after 11 months in orbit," in *IGARSS 2018 - 2018 IEEE International Geoscience and Remote Sensing Symposium*, Valencia, Spain, 2018.

[58] M. Claverie, J. Ju, J. G. Masek et al., "The harmonized Landsat and Sentinel-2 surface reflectance data set," *Remote Sensing of Environment*, vol. 219, pp. 145–161, 2018.

[59] L. Yan and D. P. Roy, "Conterminous United States crop field size quantification from multi-temporal Landsat data," *Remote Sensing of Environment*, vol. 172, pp. 67–86, 2016.

[60] Y. Cheng, A. Vrieling, F. Fava, M. Meroni, M. Marshall, and S. Gachoki, "Phenology of short vegetation cycles in a Kenyan rangeland from PlanetScope and Sentinel-2," *Environment*, vol. 248, article 112004, 2020.

[61] W. Q. Zhu, Y. Z. Pan, H. He, L. L. Wang, M. J. Mou, and J. H. Liu, "A changing-weight filter method for reconstructing a high-quality NDVI time series to preserve the integrity of vegetation phenology," *IEEE Transactions on Geoscience and Remote Sensing*, vol. 50, no. 4, pp. 1085–1094, 2012.

[62] H. Wang, R. Magagi, K. Goïta, M. Trudel, H. McNairn, and J. Powers, "Crop phenology retrieval via polarimetric SAR decomposition and Random Forest algorithm," *Remote Sensing of Environment*, vol. 231, p. 111234, 2019.

[63] C. Y. Diao, "Remote sensing phenological monitoring framework to characterize corn and soybean physiological growing stages," *Remote Sensing of Environment*, vol. 248, article 111960, 2020.

[64] B. Seyednasrollah, A. M. Young, K. Hufkens et al., "Tracking vegetation phenology across diverse biomes using Version 2.0 of the PhenoCam Dataset," *Scientific Data*, vol. 6, p. 222, 2019.

[65] "An ecosysrem phenology camera network," January 2021, https://phenocam.sr.unh.edu/webcam/network/map/.

[66] European Space Agency (ESA), "Sentinel-2 User Handbook," January 2021, https://sentinels.copernicus.eu/documents/247904/685211/Sentinel-2_User_Handbook.

[67] R. Houborg and M. F. McCabe, "A Cubesat enabled spatio-temporal enhancement method (CESTEM) utilizing Planet, Landsat and MODIS data, Landsat and MODIS data," *Remote Sensing of Environment*, vol. 209, pp. 211–226, 2018.

[68] F. Gao, J. Masek, M. Schwaller, and F. Hall, "On the blending of the Landsat and MODIS surface reflectance: predicting daily Landsat surface reflectance," *IEEE Transactions on Geoscience and Remote Sensing*, vol. 44, pp. 2207–2218, 2006.

[69] F. Gao, T. Hilker, X. Zhu et al., "Fusing Landsat and MODIS data for vegetation monitoring," *IEEE Geoscience and Remote Sensing Magazine*, vol. 3, no. 3, pp. 47–60, 2015.

[70] T. Miura, S. Nagai, M. Takeuchi, K. Ichii, and H. Yoshioka, "Improved characterisation of vegetation and land surface seasonal dynamics in Central Japan with Himawari-8 hypertemporal data," *Scientific Reports*, vol. 9, no. 1, p. 15692, 2019.

[71] Y. Qian, Z. Yang, L. Di et al., "Crop growth condition assessment at county scale based on heat-aligned growth stages," *Remote Sensing*, vol. 11, no. 20, article 2439, 2019.